


RESEARCH ARTICLE

White matter degeneration revealed by fiber-specific analysis relates to recovery of hand function after stroke

Bastian Cheng¹  | Marvin Petersen¹ | Robert Schulz¹ | Marlene Boenstrup² | Lutz Krawinkel¹ | Christian Gerloff¹ | Götz Thomalla¹

¹Klinik und Poliklinik für Neurologie, Universitätsklinikum Hamburg-Eppendorf, Hamburg, Germany

²Klinik und Poliklinik für Neurologie, Universitätsklinikum Leipzig, Leipzig, Germany

Correspondence

Bastian Cheng, Klinik und Poliklinik für Neurologie, Kopf- und Neurozentrum, Universitätsklinikum Hamburg-Eppendorf, Martinistr. 52, 20246 Hamburg, Germany. Email: b.cheng@uke.de

Funding information

German Research Foundation

Abstract

Recent developments of higher-order diffusion-weighted imaging models have enabled the estimation of specific white matter fiber populations within a voxel, addressing limitations of traditional imaging markers of white matter integrity. We applied fixel based analysis (FBA) to investigate the evolution of fiber-specific white matter changes in a prospective study of stroke patients and upper limb motor deficit over 1 year after stroke. We studied differences in fiber density and macrostructural changes in fiber cross-section. Motor function was assessed by grip strength. We conducted a whole-brain analysis of fixel metrics and predefined corticospinal tract (CST) region of interest in relation to changes in motor functions. In 30 stroke patients (mean age 62.3 years, SD ± 16.9 ; median NIHSS 4, IQR 2–5), whole-brain FBA revealed progressing loss of fiber density and cross-section in the ipsilesional corticospinal tract and long-range fiber tracts such as the superior longitudinal fascicle and trans-callosal tracts extending towards contralesional white matter tracts. Lower FBA metrics measured at the brainstem section of the CST 1 month after stroke were significantly associated with lower grip strength 3 months ($p = .009$, adjusted $R^2 = 0.259$) and 1 year (T4: $p < .001$, adj. $R^2 = 0.515$) after stroke. Compared to FA, FBA metrics showed a comparably strong association with grip strength at later time points. Using FBA, we demonstrate progressive fiber-specific white matter loss after stroke and association with functional motor outcome. Our results promote the application of fiber-specific analysis to detect secondary neurodegeneration after stroke in relation to clinical recovery.

KEYWORDS

brain ischemia, diffusion tensor imaging, magnetic resonance imaging, stroke, white matter

Abbreviations: CST, corticospinal tract; DTI, diffusion tensor imaging; FA, fractional anisotropy; FBA, fixel based analysis; FC, fiber cross-section; FD, fiber density; FOD, fiber orientation density; ROI, region of interest.

Bastian Cheng and Marvin Petersen contributed equally.

1 | INTRODUCTION

Magnetic resonance imaging (MRI) studies applying diffusion tensor imaging (DTI) have substantially contributed to understanding the

This is an open access article under the terms of the Creative Commons Attribution-NonCommercial-NoDerivs License, which permits use and distribution in any medium, provided the original work is properly cited, the use is non-commercial and no modifications or adaptations are made.

© 2021 The Authors. *Human Brain Mapping* published by Wiley Periodicals LLC.

extent of secondary white matter degeneration and associated clinical outcome after stroke (Koch, Schulz, & Hummel, 2016). In general, the degree of degeneration of corticospinal pathways such as the corticospinal tract (CST) as quantified by DTI-derived measures was shown to predict motor recovery. However, substantial improvement in motor functions also occurs despite (secondary) neurodegeneration. Although activity changes in widespread functional brain networks (Grefkes & Fink, 2020) and alterations of large-scale structural connectivity (Schlemm et al., 2021) are known to contribute to clinical recovery after stroke, the pathophysiological mechanisms underlying individual trajectories of stroke recovery are still incompletely understood, and further research is needed. Application of novel, noninvasive MRI markers in well-characterized stroke cohorts with high-quality imaging data offers an opportunity to better understand the extent and time course of structural integrity alterations after stroke.

Traditionally, DTI markers such as fractional anisotropy (FA) have been used to detect and characterize neurodegeneration after stroke (Puig et al., 2017; Schaechter et al., 2009; Wang et al., 2012). In recent years, developments of higher-order Diffusion-Weighted Imaging models such as constrained spherical deconvolution have enabled the estimation of specific white matter fiber populations within voxels, termed *fixels* (Tournier, Calamante, & Connelly, 2007). The common metrics of FBA are listed in Table 1. In summary, FBA generates scalar measures estimating the density of axons within a particular fiber population in a given voxel (“fiber density,” FD) and morphological

changes in cross-sectional areas perpendicular to fiber bundles based on registration to template images (“fiber cross section,” FC). Fixel-based analysis (FBA), a novel framework for quantifying white matter fiber properties within a voxel, has shown potential to ameliorate several shortcomings of conventional DTI measures such as FA (Mito et al., 2018; Raffelt et al., 2015; Raffelt et al., 2017; Rojas-Vite et al., 2019). FBA metrics are of increased sensitivity to white matter alterations in brain areas with complex white matter fiber architecture compared to FA. Furthermore, FBA offers a statistical framework that allows for whole-brain statistical analysis using linear models outside the boundary of traditional voxel-based analysis such as Tract-Based Spatial Statistics (Bach et al., 2014).

Changes of FBA metrics in white matter in ipsi- and contralesional white matter tracts have recently been reported in a cross-sectional study of stroke patients compared to healthy participants (Egorova et al., 2020). However, up to date, there are no reports from longitudinal studies applying FBA in prospectively collected data from stroke patients. In addition, the association of FBA metrics with the severity of clinical deficits or recovery after stroke has not been reported yet.

In this study, we apply FBA in a clinically well-defined longitudinal cohort of patients with first-time stroke and upper extremity motor deficits. Our predefined patient selection respects the clinical impact of arm and hand paresis on the most relevant daily activities and its frequent occurrence in stroke populations. In addition, loss of upper extremity function and dexterity relevantly impact on patient's independence in activities of daily living, although overall clinical severity as measured by standard stroke scales may be low (Kwakkel & Kollen, 2013).

Our study addresses two aims: First, we investigate the sensitivity of FBA-metrics to longitudinal white matter tract changes over multiple time points up to 1 year after stroke. Second, we assessed the predictive value of FBA-metrics at stroke onset regarding recovery of hand function, as studied by structural MRI using conventional DTI metrics (Koch et al., 2016). We hypothesize that longitudinal, whole-brain FBA identifies secondary white matter degeneration after stroke. In addition, we expected FBA-metrics quantified at onset in primary motor tracts to predict clinical outcome measured by grip strength after 1 year.

TABLE 1 Overview and description of metrics from fixel based analysis (FBA)

Fiber density (FD)	The FD is a measure of the fiber microarchitecture and is obtained by computing the integral of a fiber orientation distribution (FOD) amplitude. The metric corresponds to the intraaxonal volume of a fiber population, thus reflecting the actual density of fibers in a given voxel. A low FD could represent less tightly packed fibers—e.g., due to axonal loss.
Fiber-bundle cross-section (FC)	The FC is a measure of macroscopic alterations in fiber architecture obtained as a result of the registration of individual FOD images on the population template. It represents the relative change in the area of the plane perpendicular to the fiber population of interest. Decreased FC could reflect atrophy—e.g., as a result of fiber loss or demyelination.
Fiber-bundle density and cross-section (FDC)	The FDC is the product of FD and FC. Hence, the combined metric is considered to provide information about the combined pathology of microstructural and macrostructural alterations providing sensitivity to the overall capacity of a fiber population to transmit information between connected regions.

2 | METHODS

2.1 | Study design

We analyzed imaging and clinical data from the longitudinal stroke database of the Collaborative Research Centre 936 stroke cohort (2012–2017) as reported previously (Cheng et al., 2020). In summary, patients with first-time ischemic stroke were recruited 3–5 days after stroke onset via the Stroke Unit of our hospital if the following inclusion criteria were met: (1) upper limb motor deficit; (2) isolated acute ischemic stroke lesion and absence of obvious white matter lesions or lesions from previous stroke determined by magnetic resonance imaging (MRI); (3) written informed consent; (4) absence of severe

neurological or non-neurological co-morbidity. We excluded patients with evidence of preexisting structural brain damage (previous stroke, intracranial hemorrhage, any other space-occupying lesion) as determined by MRI on FLAIR and T1-weighted images. Upper limb motor deficits included arm paresis or reduced finger dexterity as reported by the patient and confirmed in clinical examination. Patients underwent MRI and clinical testing of upper extremity motor function at baseline during the acute phase (3–5 days post-stroke, T1), as well as in the subacute and chronic phases 30–40 days (T2), 85–95 days (T3), and 340–380 days (T4) after stroke. For this study, a subset of patients from the main cohort was included with (1) complete imaging data at T1 and (2) at least two additional later time points. The study was approved by the ethics committee of the chamber of physicians Hamburg, Germany (PV 37777).

2.2 | Clinical testing

For each time point (T1–T4), motor function was operationalized by grip strength in each hand using the Strength JAMAR hand evaluation kit (Elite healthcare, UK), averaging over three consecutive measurements. Proportional grip strength values (affected/unaffected hand) were used for analysis. In addition, NIHSS as a global stroke severity score and demographic data (age, sex) were recorded.

2.3 | MRI acquisition

MRI was performed at each time point (T1–T4) using a 32-channel head coil to measure both diffusion-weighted and high-resolution T1-weighted anatomical images. For diffusion-weighted imaging (DWI), 75 axial slices were obtained covering the whole brain with gradients ($b = 1,500 \text{ s/mm}^2$) applied along 64 noncollinear directions with the sequence parameters: repetition time (TR) = 10,000 ms, echo time (TE) = 82 ms, field of view (FOV) = 256×204 , slice thickness (ST) = 2 mm and in-plane resolution (IPR) = $2 \times 2 \text{ mm}^2$. The complete dataset consisted of $2 \times 64 b_{1500}$ images and one b_0 image at the beginning and one after the first 64 images. For anatomical imaging, a 3D magnetization-prepared, rapid acquisition gradient-echo sequence was used with the following parameters: TR = 2,500 ms, TE = 2.12 ms, FOV = $240 \times 192 \text{ mm}^2$, 256 axial slices, ST = 0.94 mm and IPR = $0.94 \times 0.94 \text{ mm}^2$. In addition, fluid-attenuated inversion recovery sequences were acquired in the acute phase 3–5 days after stroke for delineation of ischaemic lesions (TR = 9,000 ms, TE = 90 ms, TI = 2,500 ms, FOV = $230 \times 230 \text{ mm}^2$, ST = 5 mm and IPR = $0.7 \times 0.7 \text{ mm}^2$) and stroke lesion volumes calculated as described previously (Cheng et al., 2020).

2.4 | Data preprocessing

Imaging data was analyzed using MRTrix 3.0.1 (<http://www.mrtrix.org>), Advanced Normalization Tools (ANTs, <https://github.com/>

ANTsX/ANTs) Freesurfer 6.0.0 (<https://surfer.nmr.mgh.harvard.edu/>) and TractSeg (<https://github.com/MIC-DKFZ/TractSeg>) (Fischl, 2012; Tournier et al., 2019; Wasserthal, Neher, Hirjak, & Maier-Hein, 2019). ANTs brain extraction was used to skullstrip T1w images. DTI pre-processing included denoising, Gibbs artifacts removal, eddy current correction, correction for motion artifacts, correction of bias fields, and brain extraction (Andersson & Sotiropoulos, 2016; Kellner, Dhital, Kiselev, & Reisert, 2016; Tustison et al., 2010; Veraart et al., 2016). In addition, using ANTs' SyN registration algorithm susceptibility distortion correction has been performed by nonlinearly registering the DTI on a T1 that initially has been rigidly aligned and histogram matched with the corresponding b_0 (Avants, Epstein, Grossman, & Gee, 2008). Intracranial volume was derived from T1-weighted images using segmentations resulting from Freesurfer longitudinal analysis pipeline as described previously (Cheng et al., 2020).

2.5 | Computation of fixel metrics

Fixel metrics were computed following the recommended methodology (Raffelt et al., 2017). Upon preprocessing, response functions were estimated based on DTI and subsequently averaged over the whole sample. Single-shell three tissue constrained spherical deconvolution (SS3T-CSD) was performed to obtain fiber-orientation density (FOD) data (Dhollander & Connelly, 2016; Dhollander, Mito, Raffelt, & Connelly, 2019). Respecting the hemispheric asymmetry and fiber-specific laterality of white matter and to facilitate the assessment of potential contralesional effects, we refrained from flipping images to have all lesions on one side (Verhelst, Dhollander, Gerrits, & Vingerhoets, 2021). Instead, we split the cohort into two subgroups investigating subjects with left hemispheric and right hemispheric strokes independently. Consequently, we derived a longitudinal population template for each group adhering to an approach successfully applied previously (Genc et al., 2018). In summary, first, unbiased intraindividual templates were obtained via rigid registration of FOD images of all available time points for each subject. Then, intraindividual templates were nonlinearly registered to form a longitudinal population template. Individual FOD images of all subjects were registered on the longitudinal population template. Fiber density (FD), fiber-bundle cross-section (FC) and the fiber-bundle density and cross-section (FDC) were derived and are explained in Table 1 and Figure S1. Probabilistic tractography was performed based on the respective longitudinal population template to allow for fixel-based statistical analysis using connectivity-based fixel enhancement (Raffelt et al., 2015). Therefore, 20 million streamlines were reconstructed and filtered via spherical-deconvolution informed filtering of tractograms resulting in a whole-brain template tractogram of 2 million streamlines for each group (Smith, Tournier, Calamante, & Connelly, 2013).

See also Figure S1 for conceptual illustrations. A comprehensive discussion of the terminology of FBA metrics can be found in the original publication (Raffelt et al., 2017).

2.6 | Whole-brain fixel-based analysis

To perform FBA between different time points, general linear models were applied for each fixel as implemented in the most recent version of MRtrix3, which enables longitudinal FBA. In a paired *t*-test design, repeated measures of fixel metrics were compared between T1 and T2, T1 and T3 as well as T1 and T4 separately for patients with left- and right hemispheric stroke. To allow for smoothing and a statistical inference informed by the template tractogram, connectivity-based fixel enhancement was applied (Raffelt et al., 2015). Permutation-based correction for family-wise errors was performed on resulting *p*-values using the recommended, FWE-corrected threshold of $p < .05$ (Nichols & Holmes, 2002; Winkler, Ridgway, Webster, Smith, & Nichols, 2014).

2.7 | Corticospinal tract analysis

We investigated altered fixel density and cross-section of the CST in relation to motor functions operationalized by relative grip strength. Therefore, two regions of interest (ROI) were defined on FBA templates containing infratentorial sections of the ipsi- and contralesional CST. The CST was defined using TractSeg, a novel and robust approach to segment white matter tracts based on convolutional neural networks (Wasserthal, Neher, & Maier-Hein, 2018). CST ROIs were refined, comprising only sections at the level from the mesencephalon to the cerebral peduncle (MNI axial (*z*-) coordinates -25 to -20) as reported previously (Schulz et al., 2015). Selected fixels in predefined ROI are illustrated in Figure S2. All ROI were visually checked for accuracy, patients with brain stem stroke lesions causing direct involvement of the ROI were excluded from the analysis. Fixel metrics were averaged for each ROI. In addition, FA values were calculated and averaged in each ROI. Time- and side-dependent changes of fixel metrics ("Fixel") in CST ROI were investigated using linear mixed effect models with repeated measures (LMER): $\text{Fixel} \sim \text{Time} * \text{Side} + (1 | \text{subject}) + \text{Age} + \text{Sex}$, where "Side" refers to either ipsi- or contralesional brain regions. Time-dependent changes of relative grip strength ("Grip") were estimated by fitting an LMER adjusting for age and sex: $\text{Grip} \sim \text{Time} + (1 | \text{Subject}) + \text{Age} + \text{Sex}$. Changes of NIHSS were investigated in a separate, analogous model.

We tested the associations of relative fixel metrics and FA in CST ROI by first computing the ratio between metrics in affected and unaffected CST. We applied individual multivariable linear models for relative grip strength at T3 and T4 in relation to relative fixel metrics and FA of the CST ROI at T2 (1 month after stroke) adjusted for age and sex. Model fits were compared between models including FA and best performing fixel metric as an independent variable using the Vuong non-nested likelihood ratio test. The statistical analysis was performed in R 3.6.3 and Python 3.7.

3 | RESULTS

Complete imaging datasets at T1 and two additional time points were available for 30 of 48 patients from the main cohort. The mean age

TABLE 2 Demographic, clinical, and imaging details

	Patients (N = 30)
Mean age (years) (\pm SD)	62.3 (\pm 16.9)
Female sex (%)	11 (37%)
Lesion in left hemisphere or left brainstem (%)	18 (60%)
Median NIHSS (IQR)	4 (2–5)
Mean relative grip strength (\pm SD)	0.53 (\pm 0.35)
Mean lesion volume (ml) (\pm SD)	15.0 (\pm 23.4)
Median lesion volume (ml) (IQR)	2.2 (1.6–25.0)

was 62.3 years (SD \pm 16.9), median NIHSS was 4 (IQR 2–5). Lesions were located in the left hemisphere or left brainstem in 18 patients (60%), mean lesion volume was 15.0 mL (SD \pm 23.4 mL). Detailed demographic and clinical data are shown in Table 2.

Baseline characteristics of stroke patients at 3–5 days after stroke onset included in the study ($N = 30$). Grip strength values are presented in proportional values (affected/unaffected hand).

The anatomical distribution of stroke lesions is illustrated in Figure S3. In 3 patients (10%), stroke lesions were located at the pons, whereas the remaining lesions were located in brain areas supplied by the middle cerebral artery.

Whole-brain analysis of fixel metrics revealed significant loss of white matter over the duration of 1 month (T2), 3 months (T3), and 1 year (T4) after stroke extending beyond the side of initial ischemic stroke lesions as illustrated in Figure 1a–d. Specifically, compared to T1 (3–5 days after stroke), lower FDC, FD and FC were detected at T2 over the course of the ipsilesional CST. At T3 and T4, a significant reduction of FDC, FD and FC extended along the peripheral trajectories of the CST. In addition, at T4, there was a significant reduction of FDC and FC located in the ipsilesional superior longitudinal fascicle (SLF), transcallosal fiber tracts extending towards the contralesional precentral cortex and contralesional middle cerebellar peduncle (Figure 1e). No significant increases of the FDC, FD or FC were observed in any brain regions. Figure 2 illustrates FWE-corrected *p*-values in fixels with a significant reduction of FDC after 1 year (FEW $p < .05$) on axial cross-sections. Further detailed statistical results from FBA for all fixel metrics and group comparisons are illustrated in the supplement.

Temporal evolutions of grip strength and NIHSS are illustrated in Figure 3, showing functional improvement over time (effect of time on grip strength: $F_{3,83} = 27.5$, $p < .001$; effect of time on NIHSS: $F_{3,83} = 37.9$, $p < .001$).

For CST region of interest analysis, two patients were excluded due to missing clinical data on follow-up ($n = 1$) and stroke lesion located at the CST ROI ($n = 1$). Therefore, $n = 28$ (of $n = 30$) patients were included. Significant decrease of FDC was detected in the ipsilesional CST ROI over time (Time*Side: $F_{3,141} = 13.4$; $p < .001$), whereas no significant changes were detected at the contralesional CST ROI (Figure 4). Posthoc testing revealed significantly lower FDC for all time points after stroke ($p < .001$) compared to T1. No significant changes in FBA metrics were detected for the contralesional CST ROI. Detailed statistical results from posthoc tests can be found in Table S1.

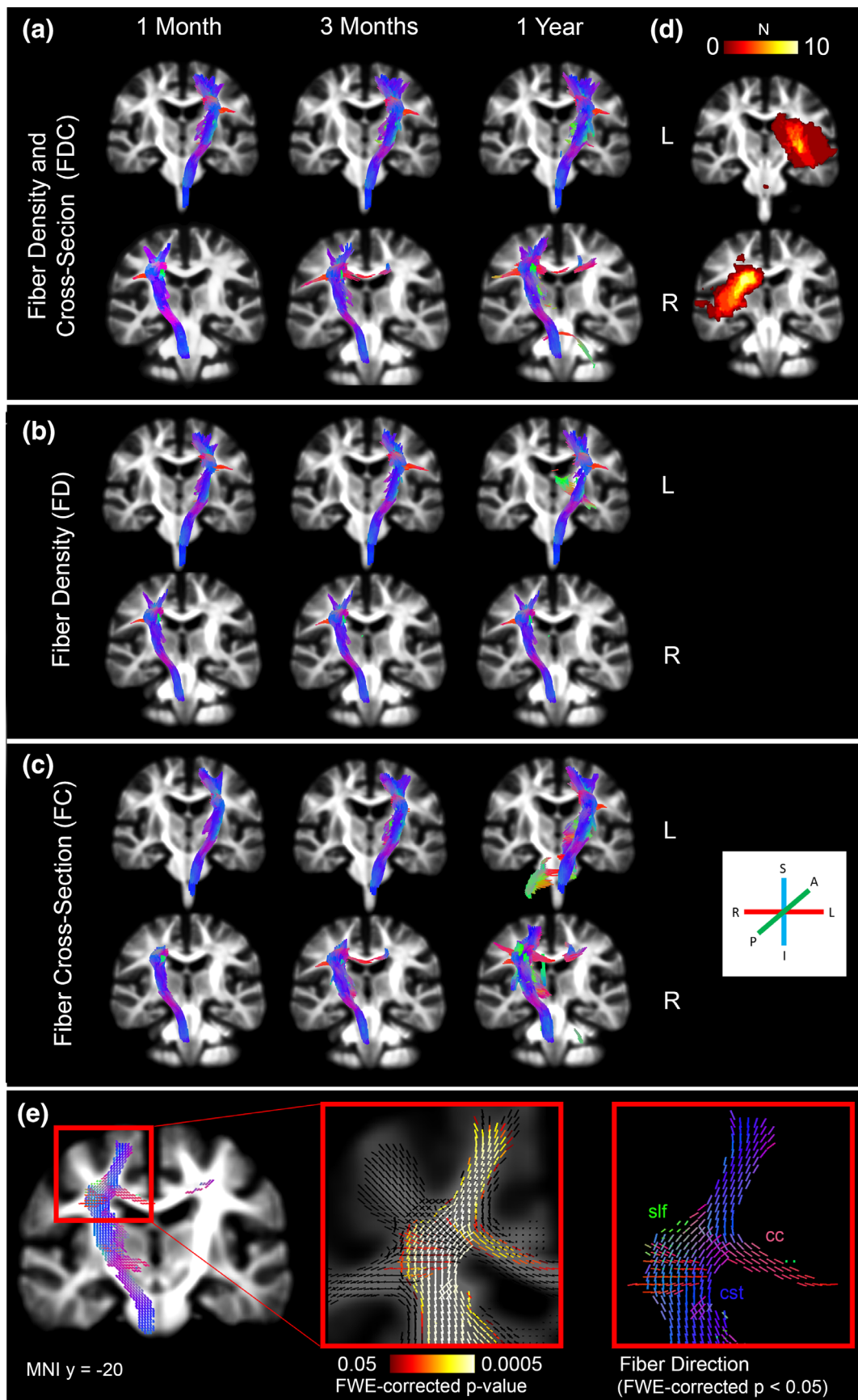


FIGURE 1 Legend on next page.

Higher relative FDC of the CST 1 month after stroke (T2) was associated with improved motor functions operationalized by relative grip strength at 3 months and 1 year after stroke ($p = .021$, adjusted $R^2 = 0.206$ and $p = .001$, adj. $R^2 = .439$). This positive association was also found for relative FD ($p = .009$, adj. $R^2 = 0.259$ and $p < .001$, adj. $R^2 = 0.515$), but not for relative FC ($p = .293$ and $p = .183$). Relative FA showed a positive association with grip strength at 3 months ($p = .003$, adj. $R^2 = 0.309$) and 1 year after stroke ($p < .001$ adj. $R^2 = 0.549$). Model fits using FBA-metrics or FA regarding the explained variance of grip strength at 3 months and 1 year were equal as shown by Vuong non-nested likelihood ratio tests (Tables S2 and S3).

4 | DISCUSSION

We applied FBA as a novel framework to quantify fiber-specific microstructural changes of white matter in a prospective cohort of stroke patients with upper limb motor deficits. Our study yielded two main results. First, whole-brain statistical analysis revealed progressive declines of FDC in several white matter tracts extending beyond regions of primary ischemic injury, most prominently in the ipsilesional corticospinal and trans-callosal tracts. Second, reduced FDC of the CST at the brainstem level was significantly related to worse motor function 3 months and 1 year after stroke. Fixel-based measures and FA as a “traditional” imaging marker of white matter integrity explained similar proportions of variance of grip strength at later time points.

In our study, we focused on patients with upper limb deficits due to the relevant clinical impact of arm and hand paresis on daily activities and its frequent occurrence in stroke populations. Furthermore, patients unable to give informed consent, that is, due to severe aphasia, were excluded. This effectively, but not intentionally, resulted in a relatively homogenous pattern of smaller, strategically located subcortical stroke lesions, which limits the generalizability of our findings to populations with larger territorial lesions and more severe clinical deficits. However, we are able to address the relevance of longitudinal changes in FBA metrics in a more specific, clinically well-characterized group of patients with relevant impairments in motor function in which high-quality MRI at multiple time points could be achieved.

In whole-brain FBA, significantly lower FDC was detected at the first follow-up, 1 month after stroke onset, over the course of

the ipsilesional CST compared to T1 (3–5 days after stroke). These changes were observable in CST sections not involved by the initial stroke lesion (Figure 1), indicative of secondary, ante- and retrograde, white matter degeneration that can most likely be explained by Wallerian degeneration after stroke resulting in axonal disintegration and consecutive atrophy of white matter fiber tracts (Rojas-Vite et al., 2019; Thomalla, Glauche, Weiller, & Röther, 2005). Predominant changes in the CST are a plausible finding considering the inclusion criteria of our study of patients with motor deficits. At later time points at 3 months and 1 year after stroke, lower FDC values were also found in more peripheral sections of the CST, the superior longitudinal fascicle and trans-callosal fiber tracts projecting to homologous, contra-lesional motor areas, in line with previous reports (Cheng et al., 2020). Lower FDC was also observed at the contralesional middle cerebellar peduncle after 1 year, potentially capturing crossed cerebellar diaschisis resulting from secondary degeneration of fiber tracts projection to the contralesional cerebellar hemisphere (Bostan, Dum, & Strick, 2013). Our findings are novel and supplement a previous cross-sectional FBA study in stroke patients showing reduced FDC 3 months after stroke throughout various white matter tracts compared to healthy participants (Egorova et al., 2020). Our findings demonstrate that FBA is sensitive to structural changes of continuous white matter disintegration after stroke (Møller et al., 2007; Wang et al., 2012).

In FBA, it is generally recommended to focus interpretation on FDC as the combined measure of FD and FC (Mito et al., 2018; Raffelt et al., 2017). Regarding changes of individual measures, we observed largely overlapping patterns of fixels demonstrating decreased FD and FC compared to T1. Interpretation of fixel metrics in isolation requires careful consideration since conceptually, atrophy subsequent to axonal loss can result in erroneously increased (or unchanged) values of FD (Raffelt et al., 2017), which is addressed by FDC as a summary measure. In our study, no significant increases of FDC, FD or FC were detected over the timeframe of 1 year after stroke. This seems expected, given that FBA metrics would most likely increase over time in the presence of increasing fractions of axonal volume as previously observed in the context of brain maturation in developing children (Genc et al., 2018). Higher values of FBA metrics were also not reported in a previous cross-sectional study of stroke patients by Egorova et al. (2020).

The application of the FBA framework in stroke research offers several advantages compared to conventional DTI tensor-based

FIGURE 1 Fiber tract-specific reductions in stroke patients from whole-brain fixel based analysis. Fiber-tract specific significant differences in fixels (colored overlays) from paired t-tests between stroke onset (T1) and 1 month (T2), 3 months (T3) and 1 year (T4) after stroke are shown, separately for (a) FDC, (b) FD, and (c) FC. (d) Illustration of lesion frequency at each original side (L: left, R: right). To enable three-dimensional visualization of all significant fixels, streamlines from the whole-brain tractogram template were cropped to include only significant fixel after family-wise error correction ($p < .05$) and colored by direction (red: left–right, blue: inferior–superior, green: anterior–posterior). Results are shown according to the analysis of patients with left- and right hemispheric stroke lesions. Detailed results exemplified in (e) illustrating test results in a brain region with a complex configuration of fiber populations (centrum semiovale) at position $y = -20$ of a corresponding template in MNI-space. Cut-out sections illustrate fixels included in the whole-brain analysis with color-coding based on FWE-corrected p -value (middle section). The right section of cut-outs illustrates directional color-coding of fixels with FWE-corrected $p < .05$ with significant results relating to specific fiber populations of the corticospinal tracts (cst), corpus callosum (cc) and superior longitudinal fascicle (slf). All images are shown in radiological orientation. FDC, fiber density and cross-section; FD, fiber density; FC, fiber cross-section

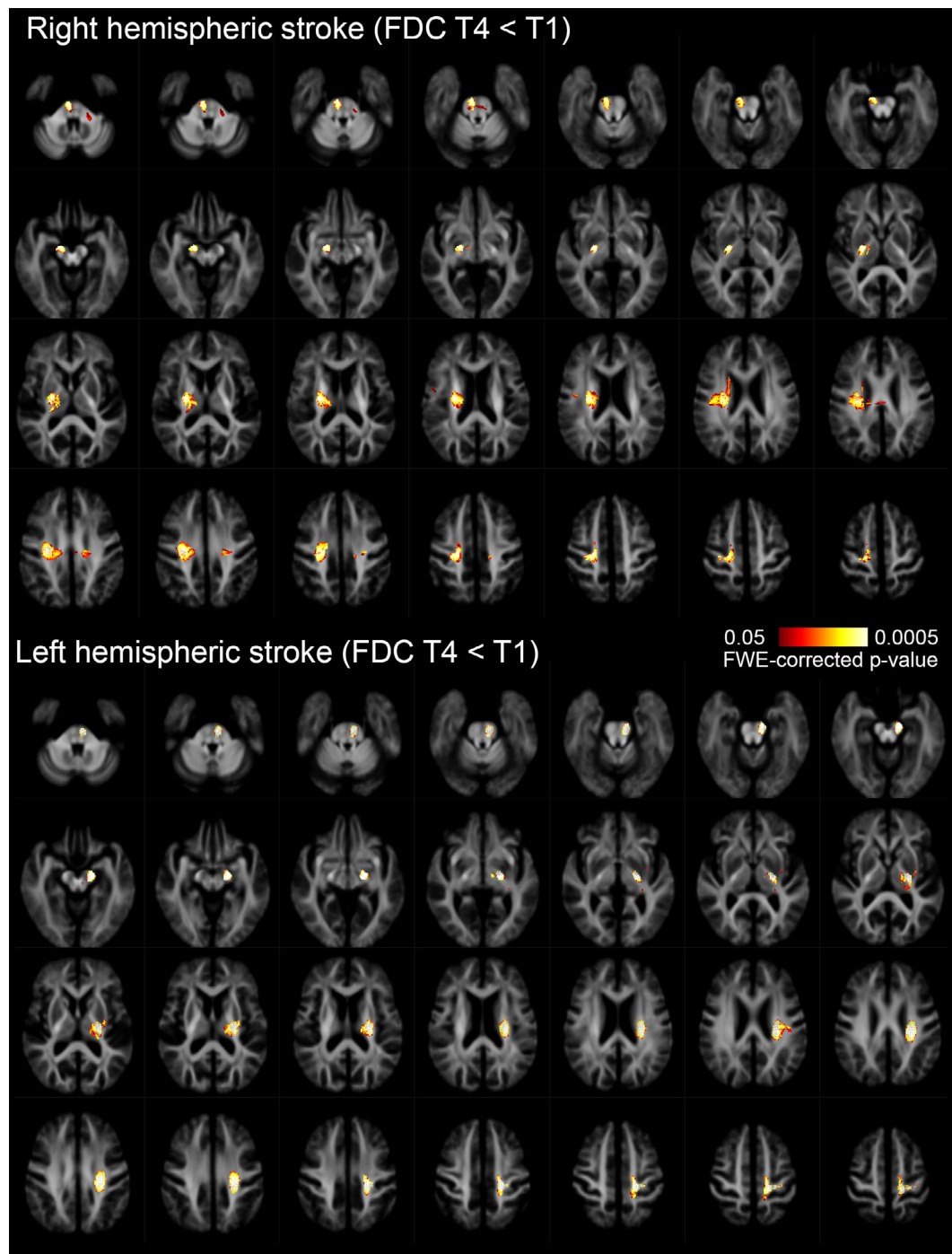


FIGURE 2 Fiber tract-specific reductions of FDC in stroke patients one year (T4) after stroke. FWE-corrected p -values from whole-brain fixel based analysis are shown for fixels with $p < .05$ on axial sections of the longitudinal group template for patients with right- and left-hemispheric stroke. All images are shown in radiological orientation. FDC, fiber density and cross-section

models. The fiber-specific model provides measures more directly interpretable regarding disturbed structural connectivity as compared to voxel-average measures such as FA. This advantage is illustrated in Figure 1e, where statistically significant changes of FDC can be related to specifically oriented fiber populations in the presence of crossing fibers at the centrum semiovale. Fixel-based comparisons promote statistical testing beyond the confinement of a white matter

“skeleton” of classical tract-based statistics, which can be limited by reduced detection accuracy compared to whole-brain analysis (Bach et al., 2014; Schwarz et al., 2014). Furthermore, FBA is helpful to guard against potential misleading findings in brain areas with complex crossing fiber architecture that are known to result in erroneously unchanged or increased values of voxel-average DTI metrics such as FA (Douaud et al., 2011; Mito et al., 2018).

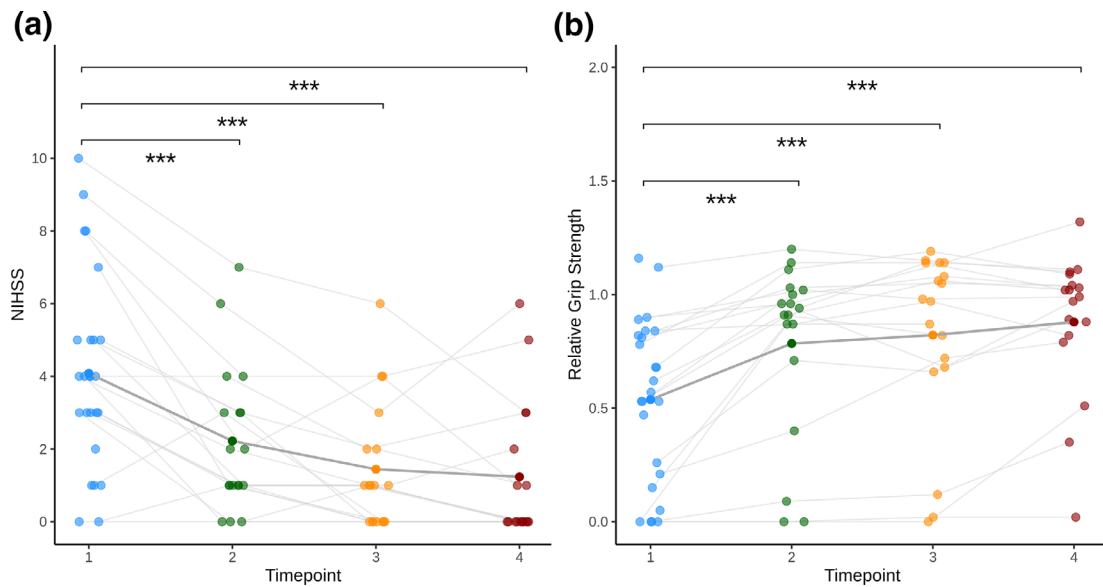


FIGURE 3 Evolution of clinical parameters. National Institutes of Health Stroke Scale (NIHSS) scores and relative grip strength (ratio affected hand/unaffected hand) are plotted against time after stroke (T1: 3–5 days; T2: 1 month; T3: 3 months, T4: 1 year). *** $p < .001$ (Bonferroni-corrected) from posthoc comparisons based on individual linear mixed effect models with repeated measures adjusted for age and sex

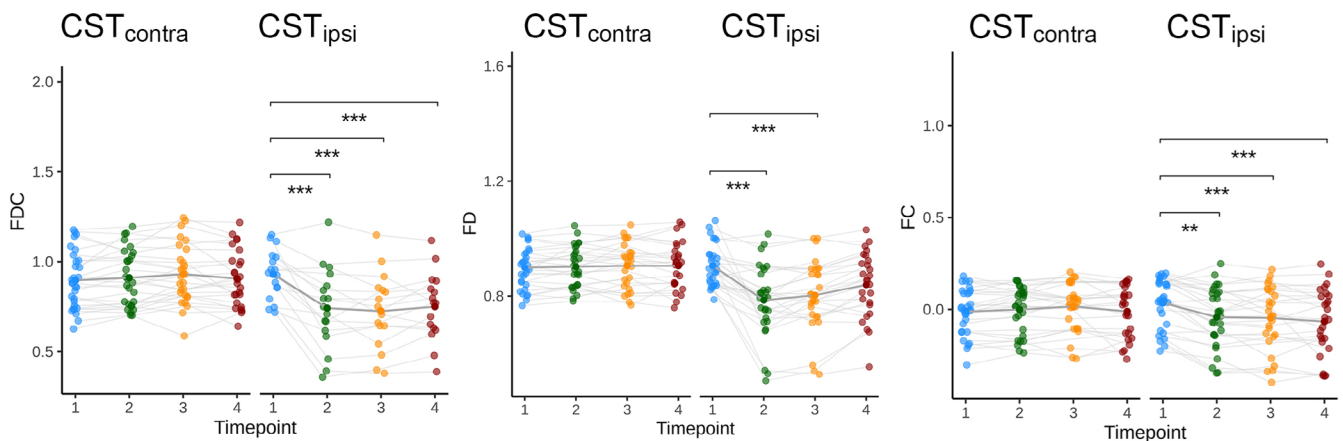


FIGURE 4 Evolution of fixel-based analysis metrics of the corticospinal tract (CST) and association with motor outcome. Evolution of fixel-based analysis metrics at the ipsilesional (“CSTipsi”) and contralesional (“CSTcontra”) CST. Individual values of FDC, FD and log-transformed FC are plotted against time stroke (T1: 3–5 days; T2: 1 month; T3: 3 months, T4: 1 year). Asterisks signify levels of statistical significance from posthoc comparisons based on individual linear mixed effect models with repeated measures adjusted for age and sex (* $p < .05$; *** $p < .001$ after Bonferroni-correction)

In addition to whole-brain statistical testing, we investigated temporal dynamics of FBA metrics of the CST in predefined brainstem areas not affected by stroke lesions. We chose this approach to allow for comparison with previous studies using a similar methodological approach (Puig et al., 2013; Puig et al., 2017). At the region of interest, FDC declined significantly over the course of 1 month after stroke onset and remained at lower levels during later time points (Figure 4). Similar trends were observed for individual FC measurements. Looking at changes of FD, we observed a dissociate, albeit nonsignificant trend with increasing values between 1 month and 1 year after stroke (Figure 4, middle section), indicating an increase in either

number, volume, or density of axons within the CST during the later time points. We speculate that differing pathophysiological processes during successive stages of Wallerian degeneration may be the underlying course for this observation (Buss et al., 2004). Whereas in initial stages, predominant loss of axons results in decreases of FD, clearance of axonal and astrocytic tissue during the later stages of degeneration leads to prominent atrophy, resulting in the continuous reduction of FC. As an alternative, methodological explanation, clearance of extracellular debris and atrophy of the fiber tracts could result in more densely packed axons and consecutively higher FD values, as discussed above (Raffelt et al., 2017).

Regarding clinical outcomes, we demonstrate a significant association between the CST-FDC 1 month after stroke and relative grip strength measured after 3 months and 1 year. Therefore, we demonstrate that FBA metrics at the early subacute phase after stroke are of value as a prognostic marker for upper extremity motor outcome. Our findings are in line with the known dependency of motor recovery on CST structural integrity (Puig et al., 2010; Puig et al., 2013). When exploring results relating to individual FBA metrics, motor outcome at T3 and T4 were significantly related to FD, whereas no significant association was detected for FC (after Bonferroni-correction). These observations suggest that, compared with FC, FD is superior sensitivity as an imaging marker of CST integrity for predicting motor functions. This would be plausible from a conceptual and pathophysiological point of view since FD is a measure specifically susceptible to a changed density of axons, whereas FC predominantly captures cross-voxel morphological changes of white matter, including extra-axonal brain tissue. Compared to FA as a “traditional” parameter of white matter integrity, FBA metrics, specifically, FD, explained a similar amount of variance of clinical outcome in our group of patients. However, none of the FBA-metrics were superior to FA in predicting grip strength at later time points. This negative finding most likely results from our pre-specified selection of patients with upper extremity motor deficits and consecutive involvement and degeneration of the CST. Given the relatively homogenous fiber orientations with a scarce amount of crossing white matter tracts in the CST at the brainstem level, it is conceivable that FA values in our measurements are not relevantly confounded by crossing fiber architectures. Therefore, it is possible that the full potential and technical advantage of FBA, namely the resolution and analysis of multiple principle fiber orientations, was not fully exploited at this section. Therefore, future studies involving patients with deficits in more distributed brain functions such as language, spatial orientation or cognition, are needed to further explore the predictive value of FBA metrics. As an additional limitation, we analyzed data from a well-defined and particular population of stroke patients with upper extremity motor deficits and comparatively small stroke lesion volumes. Whereas these selection criteria increase the interpretability and relevance of our findings for patients with relevant clinical deficits due to strategically located lesions, it limits the generalizability to more diverse stroke populations with larger infarct volumes.

In conclusion, in a prospective study of patients with motor deficits after stroke, we demonstrate progressive, fiber-specific loss of white matter at ipsi- and contralesional white matter tracts using a novel framework of FBA. Lower FDC, capturing decreased corticospinal tract integrity, was related to worse functional motor outcomes to an extent comparable with FA. Our results promote the application of fiber-specific analysis to detect secondary neurodegeneration after stroke in relation to clinical recovery.

ACKNOWLEDGMENTS

This research was supported by the German Research Foundation (DFG) SFB 936 “Multi-site Communication in the Brain” (project C1

and C2). Open Access funding enabled and organized by Projekt DEAL.

CONFLICT OF INTEREST

The authors declare no conflicts of interest.

DATA AVAILABILITY STATEMENT

Anonymized and selected imaging data is available to qualified researchers upon reasonable request. Scripts for data analysis are available at a public repository (<https://github.com/csi-hamburg/>).

ORCID

Bastian Cheng  <https://orcid.org/0000-0003-2434-1822>

REFERENCES

- Andersson, J. L. R., & Sotiropoulos, S. N. (2016). An integrated approach to correction for off-resonance effects and subject movement in diffusion MR imaging. *NeuroImage*, 125, 1063–1078.
- Avants, B., Epstein, C., Grossman, M., & Gee, J. (2008). Symmetric diffeomorphic image registration with cross-correlation: Evaluating automated labeling of elderly and neurodegenerative brain. *Medical Image Analysis*, 12, 26–41.
- Bach, M., Laun, F. B., Leemans, A., Tax, C. M. W., Biessels, G. J., Stieltjes, B., & Maier-Hein, K. H. (2014). Methodological considerations on tract-based spatial statistics (TBSS). *NeuroImage*, 100, 358–369.
- Bostan, A. C., Dum, R. P., & Strick, P. L. (2013). Cerebellar networks with the cerebral cortex and basal ganglia. *Trends in Cognitive Sciences*, 17, 241–254.
- Buss, A., Brook, G. A., Kakulas, B., Martin, D., Franzen, R., Schoenen, J., ... Schmitt, A. B. (2004). Gradual loss of myelin and formation of an astrocytic scar during Wallerian degeneration in the human spinal cord. *Brain*, 127, 34–44.
- Cheng, B., Dietzmann, P., Schulz, R., Boenstrup, M., Krawinkel, L., Fiehler, J., ... Thomalla, G. (2020). Cortical atrophy and transcallosal diaschisis following isolated subcortical stroke. *Journal of Cerebral Blood Flow and Metabolism*, 40, 611–621.
- Dhollander, T., & Connelly, D. R. (2016). A novel iterative approach to reap the benefits of multi-tissue CSD from just single-shell ($+ b = 0$) diffusion MRI data A novel iterative approach to reap the benefits of multi-tissue CSD. *Proc 24th Annu Meet Int Soc Magn Reson Med*: 3010.
- Dhollander, T., Mito, R., Raffelt, D., & Connelly, A. (2019). Improved white matter response function estimation for 3-tissue constrained spherical deconvolution. *Proc 27th Annu Meet Int Soc Magn Reson Med May*:555.
- Douaud, G., Jbabdi, S., Behrens, T. E. J., Menke, R. A., Gass, A., Monsch, A. U., ... Smith, S. (2011). DTI measures in crossing-fibre areas: Increased diffusion anisotropy reveals early white matter alteration in MCI and mild Alzheimer's disease. *NeuroImage*, 55, 880–890.
- Egorova, N., Dhollander, T., Khelif, M. S., Khan, W., Werden, E., & Brodtmann, A. (2020). Pervasive white matter fiber degeneration in ischemic stroke. *Stroke*, 51, 1507–1513.
- Fischl, B. (2012). FreeSurfer. *NeuroImage*, 62, 774–781.
- Genc, S., Smith, R. E., Malpas, C. B., Anderson, V., Nicholson, J. M., Efron, D., ... Silk, T. J. (2018). Development of white matter fibre density and morphology over childhood: A longitudinal fixel-based analysis. *NeuroImage*, 183, 666–676.
- Grefkes, C., & Fink, G. R. (2020). Recovery from stroke: Current concepts and future perspectives. *Neurological Research and Practice*, 2, 17.
- Kellner, E., Dhital, B., Kiselev, V. G., & Reisert, M. (2016). Gibbs-ringing artifact removal based on local subvoxel-shifts. *Magnetic Resonance in Medicine*, 76, 1574–1581.

- Koch, P., Schulz, R., & Hummel, F. C. (2016). Structural connectivity analyses in motor recovery research after stroke. *Annals of Clinical Translational Neurology*, 3, 233–244.
- Kwakkel, G., & Kollen, B. J. (2013). Predicting activities after stroke: What is clinically relevant? *International Journal of Stroke*, 8, 25–32.
- Mito, R., Raffelt, D., Dhollander, T., Vaughan, D. N., Tournier, J. D., Salvado, O., ... Connelly, A. (2018). Fibre-specific white matter reductions in Alzheimer's disease and mild cognitive impairment. *Brain*, 141, 888–902.
- Møller, M., Frandsen, J., Andersen, G., Gjedde, A., Vestergaard-Poulsen, P., & Østergaard, L. (2007). Dynamic changes in corticospinal tracts after stroke detected by fibretracking. *Journal of Neurology, Neurosurgery, and Psychiatry*, 78, 587–592.
- Nichols, T. E., & Holmes, A. P. (2002). Nonparametric permutation tests for functional neuroimaging: A primer with examples. *Human Brain Mapping*, 15, 1–25.
- Puig, J., Blasco, G., Daunis-I-Estadella, J., Thomalla, G., Castellanos, M., Figueras, J., ... Pedraza, S. (2013). Decreased corticospinal tract fractional anisotropy predicts long-term motor outcome after stroke. *Stroke*, 44, 2016–2018.
- Puig, J., Blasco, G., Schlaug, G., Stinear, C. M., Daunis-i-Estadella, P., Biarnes, C., ... Pedraza, S. (2017). Diffusion tensor imaging as a prognostic biomarker for motor recovery and rehabilitation after stroke. *Neuroradiology*, 59, 343–351.
- Puig, J., Pedraza, S., Blasco, G., Daunis-i-Estadella, J., Prats, A., Prados, F., ... Serena, J. (2010). Wallerian degeneration in the corticospinal tract evaluated by diffusion tensor imaging correlates with motor deficit 30 days after middle cerebral artery ischemic stroke. *American Journal of Neuroradiology*, 31, 1324–1330.
- Raffelt, D. A., Smith, R. E., Ridgway, G. R., Tournier, J.-D., Vaughan, D. N., Rose, S., ... Connelly, A. (2015). Connectivity-based fixel enhancement: Whole-brain statistical analysis of diffusion MRI measures in the presence of crossing fibres. *NeuroImage*, 117, 40–55.
- Raffelt, D. A., Tournier, J.-D., Smith, R. E., Vaughan, D. N., Jackson, G., Ridgway, G. R., & Connelly, A. (2017). Investigating white matter fibre density and morphology using fixel-based analysis. *NeuroImage*, 144, 58–73.
- Rojas-Vite, G., Coronado-Leija, R., Narvaez-Delgado, O., Ramírez-Manzanares, A., Marroquín, J. L., Noguez-Imm, R., ... Concha, L. (2019). Histological validation of per-bundle water diffusion metrics within a region of fiber crossing following axonal degeneration. *NeuroImage*, 201, 116013.
- Schaechter, J. D., Fricker, Z. P., Perdue, K. L., Helmer, K. G., Vangel, M. G., Greve, D. N., & Makris, N. (2009). Microstructural status of ipsilesional and contralesional corticospinal tract correlates with motor skill in chronic stroke patients. *Human Brain Mapping*, 30, 3461–3474.
- Schlemm, E., Ingwersen, T., Königsberg, A., Boutitie, F., Ebinger, M., Endres, M., ... Cheng, B. (2021). Preserved structural connectivity mediates the clinical effect of thrombolysis in patients with anterior-circulation stroke. *Nature Communications*, 12, 2590.
- Schulz, R., Koch, P., Zimerman, M., Wessel, M., Bönstrup, M., Thomalla, G., ... Hummel, F. C. (2015). Parietofrontal motor pathways and their association with motor function after stroke. *Brain*, 138, 1949–1960.
- Schwarz, C. G., Reid, R. I., Gunter, J. L., Senjem, M. L., Przybelski, S. A., Zuk, S. M., ... Jack, C. R. (2014). Improved DTI registration allows voxel-based analysis that outperforms tract-based spatial statistics. *NeuroImage*, 94, 65–78.
- Smith, R. E., Tournier, J.-D., Calamante, F., & Connelly, A. (2013). SIFT: Spherical-deconvolution informed filtering of tractograms. *NeuroImage*, 67, 298–312.
- Thomalla, G., Glauche, V., Weiller, C., & Röther, J. (2005). Time course of wallerian degeneration after ischaemic stroke revealed by diffusion tensor imaging. *Journal of Neurology, Neurosurgery, and Psychiatry*, 76, 266–268.
- Tournier, J.-D., Calamante, F., & Connelly, A. (2007). Robust determination of the fibre orientation distribution in diffusion MRI: Non-negativity constrained super-resolved spherical deconvolution. *NeuroImage*, 35, 1459–1472.
- Tournier, J.-D., Smith, R., Raffelt, D., Tabbara, R., Dhollander, T., Pietsch, M., ... Connelly, A. (2019). MRtrix3: A fast, flexible and open software framework for medical image processing and visualisation. *NeuroImage*, 202, 116137.
- Tustison, N. J., Avants, B. B., Cook, P. A., Zheng, Y., Egan, A., Yushkevich, P. A., & Gee, J. C. (2010). N4ITK: Improved N3 bias correction. *IEEE Transactions on Medical Imaging*, 29, 1310–1320.
- Veraart, J., Novikov, D. S., Christiaens, D., Ades-aron, B., Sijbers, J., & Fieremans, E. (2016). Denoising of diffusion MRI using random matrix theory. *NeuroImage*, 142, 394–406.
- Verhelst, H., Dhollander, T., Gerrits, R., & Vingerhoets, G. (2021). Fibre-specific laterality of white matter in left and right language dominant people. *NeuroImage*, 230, 117812.
- Wang, L. E., Tittgemeyer, M., Imperati, D., Diekhoff, S., Ameli, M., Fink, G. R., & Grefkes, C. (2012). Degeneration of corpus callosum and recovery of motor function after stroke: A multimodal magnetic resonance imaging study. *Human Brain Mapping*, 33, 2941–2956.
- Wasserthal, J., Neher, P., & Maier-Hein, K. H. (2018). TractSeg – Fast and accurate white matter tract segmentation. *NeuroImage*, 183, 239–253.
- Wasserthal, J., Neher, P. F., Hirjak, D., & Maier-Hein, K. H. (2019). Combined tract segmentation and orientation mapping for bundle-specific tractography. *Medical Image Analysis*, 58, 101559.
- Winkler, A. M., Ridgway, G. R., Webster, M. A., Smith, S. M., & Nichols, T. E. (2014). Permutation inference for the general linear model. *NeuroImage*, 92, 381–397.

SUPPORTING INFORMATION

Additional supporting information may be found in the online version of the article at the publisher's website.

How to cite this article: Cheng, B., Petersen, M., Schulz, R., Boenstrup, M., Krawinkel, L., Gerloff, C., & Thomalla, G. (2021). White matter degeneration revealed by fiber-specific analysis relates to recovery of hand function after stroke. *Human Brain Mapping*, 42(16), 5423–5432. <https://doi.org/10.1002/hbm.25632>